Essential Readings in Light Metals: Aluminum Reduction Technology.
Edited by Geoff Bearne, Marc Dupuis and Gary Tarcy.

Anodic Overpotentials in the Electrolysis of Alumina

B. J. WELCH and N. E. RICHARDS

Reynolds Metals Company, Sheffield, Alabama

Abstract

Overpotentials for the anodic reaction in the electrolysis of alumina dissolved in molten fluoride electrolytes have been measured by a steady state technique using C, CO_2 + $CO/Al_2O_3(l)$ reference electrode. Overpotentials for the discharge of oxygen-containing anions in the systems Na_3AlF_6 + CaF_2 + Al_2O_3 and Na_3AlF_6 + Li_3AlF_6 + Al_2O_3 are reported as a function of current density, temperature, and solvent composition. The linear portion of the Tafel curves extends over approximately 1.5 powers of ten in current density. The slopes are independent of solvent. The heat of activation evaluated from the temperature dependence is 13 ± 4 kcal/mole, which is in excellent agreement with the value determined by potentiostatic means. A theoretical kinetic analysis of possible anodic reactions leading to the evolution of CO_2 is presented. In each of the possible routes it appears that the rate-determining step is a two-electron transfer reaction in which oxide ions or oxygen-containing anions are discharged.

Introduction

Studies of anode overpotentials in molten salt systems, in general, and in molten fluoride systems, in particular, have been limited. The published data on the anode overpotential in the Hall-Heroult cell using molten cryolite-alumina[1,2] can be criticized due to the lack of suitable reference electrodes and the inadequate precautions taken to insure the removal of impurities from the electrolyte which affect the anode process.

Earlier investigations in this program[3] have established that the reference electrode CO_2 + $CO(O_2)$, $C|Na_3AlF_6$ + Al_2O_3 is reversible and can be employed satisfactorily as a reference electrode for overpotential studies in the electrolysis of liquid Na_3AlF_6 + Al_2O_3 mixtures.[4]

Anodic polarization curves for the electrolytic decomposition of Al_2O_3 in cryolitic solvents of different compositions have been determined from the measurement of the anode-reference electrode potentials over a wide range of current density. Interpretation of the electrode kinetics is discussed with respect to possible mechanisms for the evolution of CO_2 at the carbon anode.

Experimental Apparatus

A schematic diagram of the experimental assembly used for the overpotential measurements is shown in Figure 1. The cell consisted of the working anode (*A,B,P,J*), surrounded by a shell (*E,L*), the counter electrode or cathode (*D,I*), combination auxiliary anode and stirrer (*C,H,K*), and the reference electrode (*M,N,O,Q,R,S*). The steady state reversible potential of the anode and reference electrode, i.e., under conditions of no net current flow, was established by flowing a gas mixture of CO_2 and CO through their respective carbon electrodes (*J,S*), and into contact with the melt. The tube *E* permitted the collection of the gases passing over the anode and led to the infrared analyzing system. The support rods which also served as electrical contact leads (*B,C,D,N*), were of Inconel tubing, which after initial superficial attack was inert to the condensate from the electrolyte. The support tubes *M* and gas collection skirt (*E,L*) were also made from Inconel tubing. An insulated platinum probe *A*, was used to eliminate the ohmic potential difference (p.d.) along the anode support from the anode reference p.d.

The molten electrolyte was contained in a graphite crucible *F*. This was supported by, but insulated from, an Inconel cylinder *G*. The electrode assembly and loaded crucible were sealed in the tube of a Kanthal wire resistance furnace. This furnace had a uniform temperature zone 4 in. in length (obtained by means of external resistance shunts) and at thermal equilibrium the temperature was controlled to ±0.2°C by a system which included a recording potentiometer fitted with a retransmitting slidewire, a Leeds & Northrup C.A.T. proportional action unit with feedback, a magnetic amplifier, and a saturable reactor.

For all experimental measurements the geometry of the exposed anode surface area was constant. No attempts were made to determine the true surface area and results are reported in terms of apparent (or geometric) current density. This does not affect the interpretation of results with respect to the Tafel equation[5] since, if r is the ratio between the true and geometric surface areas, then we have

$$\eta = a + \frac{RT}{\alpha F}\log i$$
$$= a + \frac{RT}{\alpha F}\log\frac{i'}{r}$$
$$= a' + \frac{RT}{\alpha F}\log i'$$

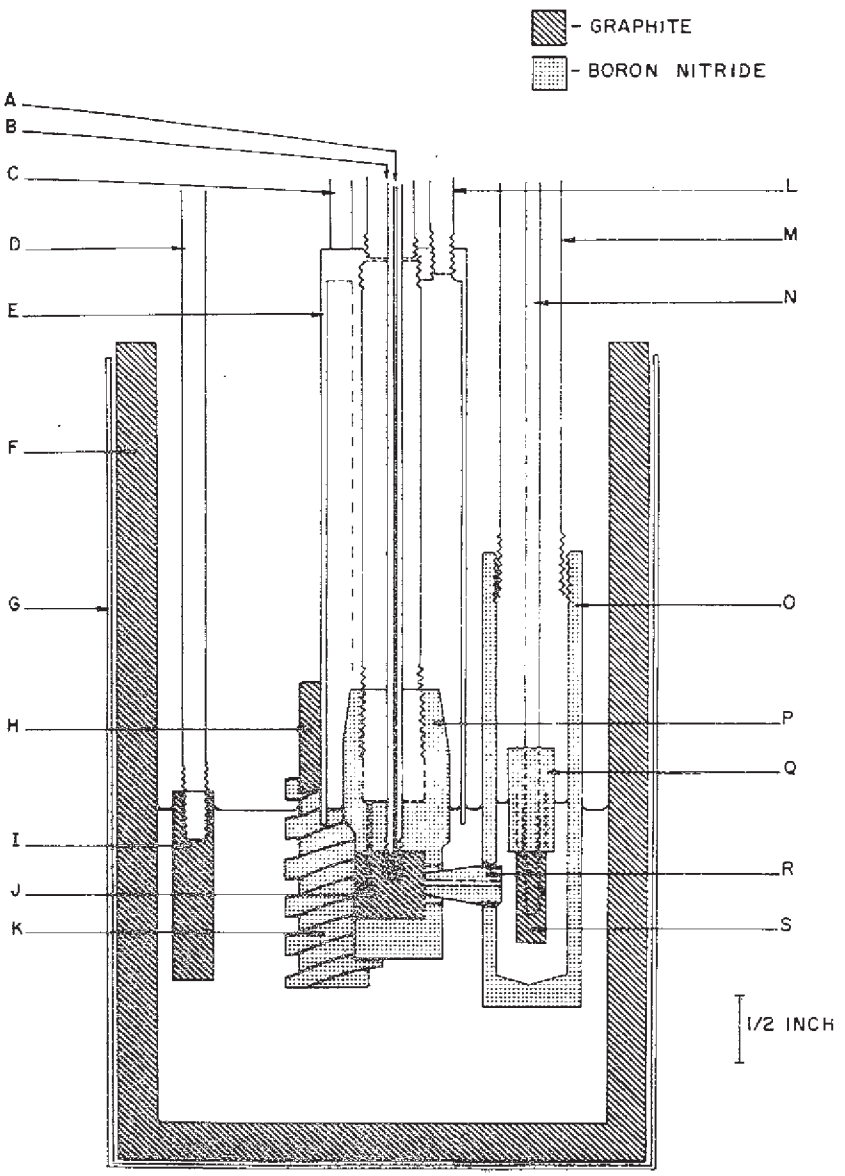

Fig. 1. Schematic diagram of the cell.

where η is the overpotential, a and a' are constants, i is the true current density, and i' is the apparent current density. Since the kinetic consideration of electrode processes depends on the evaluation of $RT/\alpha F$ and this value is not altered by the ratio of true to geometric surface areas, it is apparent that it is not necessary to determine the true surface area from a mechanistic viewpoint.

Materials

The cryolite was prepared from hand-selected lumps of Greenland cryolite which were crushed and washed with HCl. British Drug House Analar grade alumina was used. The LiF, AlF_3, and CaF_2 were Baker's analyzed reagent grade chemicals.

All the salts were dried at 110°C prior to use and salt mixtures of the required composition were synthesized by accurate weighing.

The CO_2 + CO gas mixtures were obtained from cylinders prepared from specifications submitted by Matheson and Co. The components were 99.98% and 99.5% minimum purity, respectively.

AUC grade graphite (National Carbon) was used as anode material for all experimental measurements. Earlier investigations of overpotentials in the Na_3AlF_6 + Al_2O_3 system[4] using anodes of AUC and ZTA graphites as well as coke carbon gave identical Tafel slopes.[5] Because of its good machining properties, AUC graphite was chosen as the anode material for this particular research.

Experimental Procedure

Potential measurements were made by the direct method. The electrical circuit was fundamentally the same as that used by Janz and Saegusa.[6] In this work, the polarizing current was supplied from a Solavolt stabilized adjustable dc power supply. The anode-reference potential was measured on the Y axis of a Moseley model 2A autograph X-Y recorder. The p.d. across a current-measuring shunt was fed into a Moseley logarithmic converter unit, the output of which was connected to the X axis of the X-Y recorder.

At all times CO_2 + CO gas mixtures were impressed on both the reference electrode and the working anode to establish steady state reversible potentials. Before polarization measurements were made, the electrolyte was pre-electrolyzed using the auxiliary electrode to remove anodically deposited impurities from the bath. When this procedure was completed, the auxiliary electrode was raised from the bath to prevent dissolution of impurities. An atmosphere of argon was kept in the sealed furnace tube at all times.

Experimental measurements were made by increasing the current in stepwise increments and recording changes in anode-reference electrode p.d. and current density logarithmically.

It had been established earlier[4] that for any change in current, the anode-reference p.d. attains its steady state value almost instantaneously.

Results

Anodic overpotentials for the electrolytic decomposition of alumina at a carbonaceous anode were determined with several partial pressures of CO_2 in cryolite solvents represented by $3Na_3AlF_6 + CaF_2$, $2Na_3AlF_6$, and $Na_3AlF_6 + Li_3AlF_6$. The concentration of alumina was 17.1 mole-% in all of these electrolytes. The experimental measurements were carried out in the temperature range of 960 to 1030°C.

The System Na_3AlF_6–CaF_2–Al_2O_3

In the mixture investigated, the CaF_2 to cryolite ratio was similar to that used in industrial reduction cells. The composition of the liquid electrolytes used in these experiments expressed as weight percentages

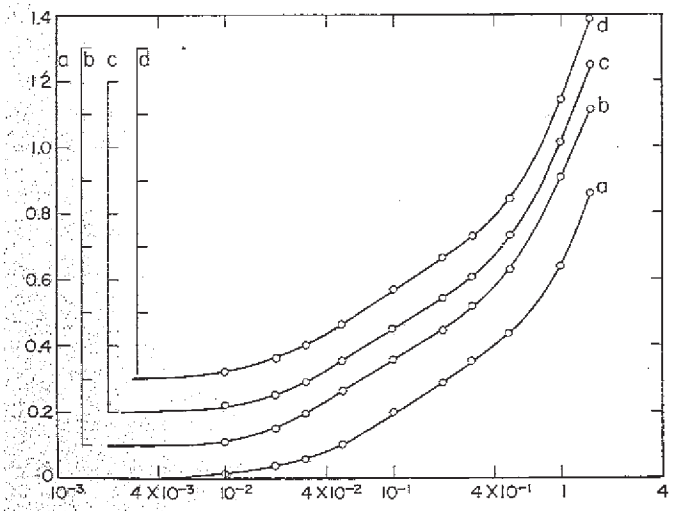

Fig. 2. Relation between anode overpotential and log current density for Al_2O_3 in $3Na_3AlF_6 + CaF_2$ at 1010 ± 1°C with anode gas containing *a*, 67% CO_2; *b*, 55% CO_2; *c*, 39% CO_2; and *d*, 20% CO_2. Ordinate: overpotential (volts). Abscissa: current density (amp cm^{-2}).

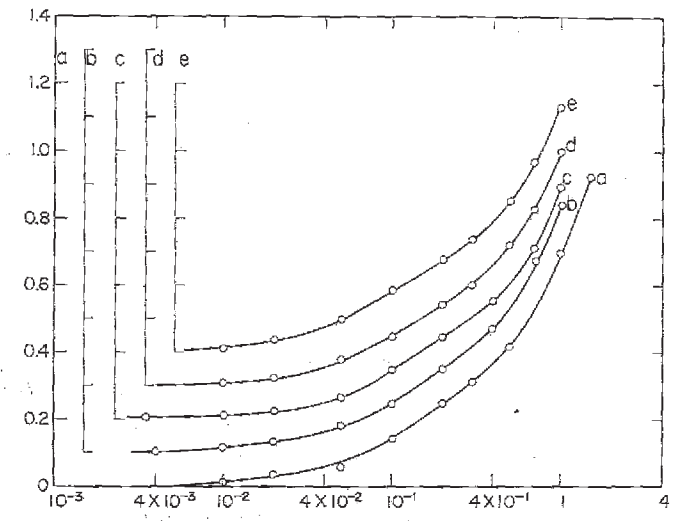

Fig. 3. Isotherms of anode overpotential in the electrolysis of Al_2O_3 in the solvent $3Na_3AlF_6 + CaF_2$ with 65% CO_2 in anode gas. *a*, 1025°C; *b*, 1010°C; *c*, 999°C; *d*, 990°C; and *e*, 973°C. Ordinate: overpotential (volts). Abscissa: current density (amp cm^{-2}).

was $82.62Na_3AlF_6$, $7.62CaF_2$, and $9.76Al_2O_3$. Overpotential measurements were made as a function of current density (c.d.) at 1010 ± 1°C with different CO + CO_2 mixtures impressed on the anode, and the results are presented in Figure 2. Tafel curves obtained at different temperatures but with the same steady state gas composition (65% CO_2 +

TABLE I
Tafel Constants and Exchange Currents for the Anodic Process on Graphite in the Electrolyte Na_3AlF_6-CaF_2-Al_2O_3

Temp., °C	Compn. of CO_2 + CO gas CO_2, %	Tafel constants *a*	Tafel constants *b*	Exchange current, amp cm^{-2}
1011	67	0.524	0.335	0.0250
1010	55	0.568	0.315	0.0175
1010	39	0.572	0.320	0.0170
1010	20	0.602	0.330	0.0160
1025	65	0.580	0.340	0.041
1010	65	0.596	0.340	0.038
999	65	0.572	0.330	0.036
990	65	0.566	0.320	0.032
973	65	0.595	0.325	0.028

35% CO) at the anode-melt interface are shown in Figure 3. The current independent terms of the Tafel equation, $\eta = a + b \log i$, which represent the linear portion of the curves in Figures 2 and 3, and the corresponding exchange currents (i_0) are summarized in Table I.

The current density at which the anode effect occurs in this electrolyte was also measured. At 1010°C this phenomenon occurred at 13.5 amp cm^{-2} which corresponds to a limiting current density (i_L) of 5.8 amp cm^{-2}.

The Systems Na_2LiAlF_6–Al_2O_3 and $(NaLi)_{3/2}AlF_6$–Al_2O_3

The compositions of the two electrolytes containing LiF in which anode overpotentials were measured expressed in terms of weight percentage were 65.4Na_3AlF_6, 12.9AlF_3, 11.93LiF, 9.77Al_2O_3, and 49.3Na_3AlF_6, 20.9AlF_3, 19.4LiF, and 10.4, respectively. The experimental η — log i curves at temperature 1010°C for a series of CO_2 + CO gas mixtures on the electrode are reproduced in Figures 4 and 6 in each of which the overpotential ordinate is translated successively by 0.1 to avoid superposition. Isotherms of overpotential over a range of current densities are plotted in Figures 5 and 7 for the 27.2 mole-% Li_3AlF_6 and 41.5

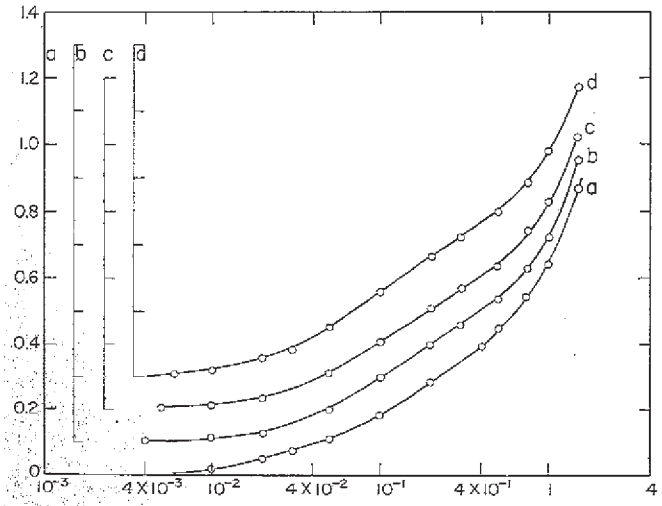

Fig. 4. Plot of anode overpotential versus log current density for Al_2O_3 in $2Na_3AlF_6$ + Li_3AlF_6 at 1010°C with anode gas containing, *a*, 85% CO_2; *b*, 67% CO_2; *c*, 44% CO_2; and *d*, 18% CO_2. Ordinate: overpotential (volts). Abscissa: current density (amp cm^{-2}).

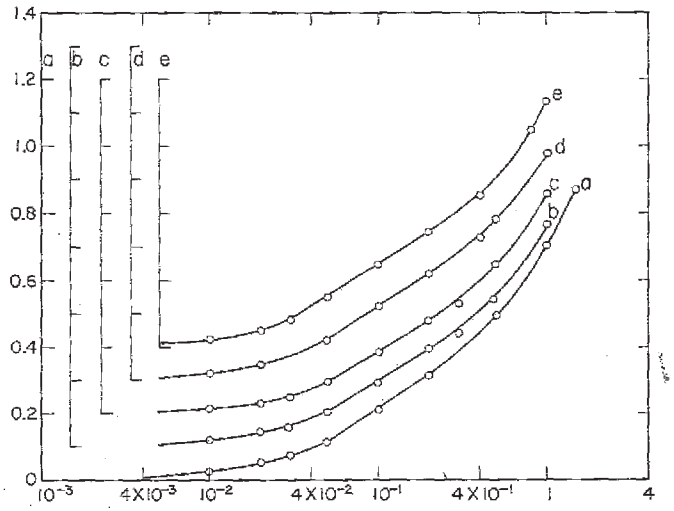

Fig. 5. Isotherms of anode overpotential in the electrolysis of Al_2O_3 in solvent $2Na_3AlF_6$ + Li_3AlF_6 with 45% CO_2 in anode gas. *a*, 1030°C; *b*, 997°C; *c*, 985°C; *d*, 960°C; and *e*, 950°C. Ordinate: overpotential (volts). Abscissa: current density (amp cm^{-2}).

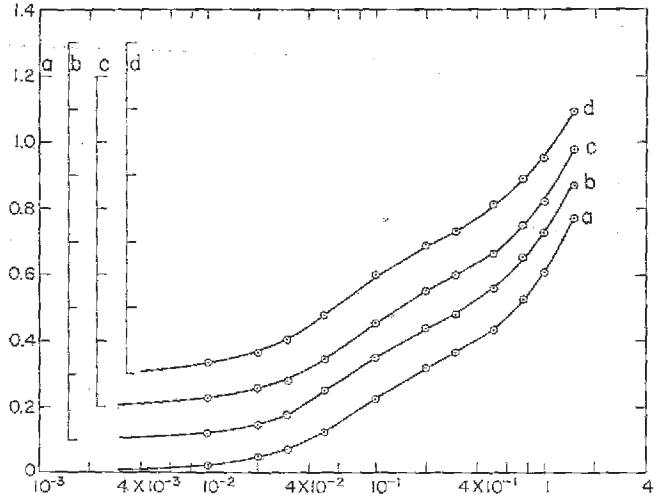

Fig. 6. Relation between anode overpotential and log current density for Al_2O_3 in Na_3AlF_6 + Li_3AlF_6 at 1010°C with anode gas containing, *a*, 82% CO_2; *b*, 58% CO_2; *c*, 40% CO_2; and *d*, 20% CO_2. Ordinate: overpotential (volts). Abscissa: current density (amp cm^{-2}).

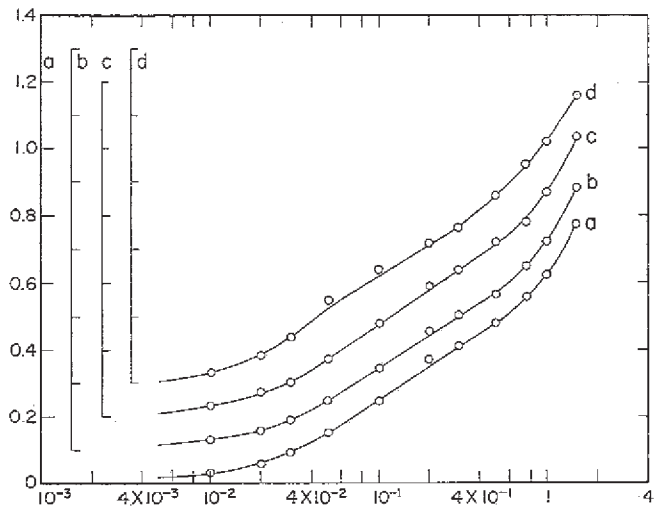

Fig. 7. Isotherms of anode overpotential in the electrolysis of Al_2O_3 in the solvent Na_3AlF_6 + Li_3AlF_6 with 40 ± 1% CO_2 in anode gas. *a*, 1020°C; *b*, 1015°C; *c*, 989°C; and *d*, 967°C. Ordinate: overpotential (volts). Abscissa: current density (amp cm^{-2}).

TABLE II
Tafel Constants and Exchange Currents for the Anodic Process on Graphite in Electrolytes of the System Na_3AlF_6-Li_3AlF_6-Al_2O_3

Li_3AlF_6, mole-%	Temp., °C	Compn. of CO_2 + CO gas CO_2, %	Tafel constants *a*	*b*	Exchange current, amp cm^{-2}
27.2	1010	85	0.522	0.330	0.0290
	1010	67	0.533	0.335	0.0270
	1010	44	0.525	0.330	0.0230
	1010	18	0.600	0.335	0.0185
	1030	45	0.550	0.340	0.0290
	997	45	0.520	0.325	0.0260
	985	45	0.503	0.325	0.0250
	960	45	0.542	0.320	0.0215
	950	45	0.570	0.320	0.0185
41.5	1010	82	0.530	0.320	0.0210
	1010	58	0.548	0.320	0.0180
	1010	40	0.560	0.320	0.0170
	1010	20	0.600	0.325	0.0145
	1020	40	0.575	0.330	0.0185
	1015	40	0.560	0.320	0.0170
	989	40	0.605	0.325	0.0155
	967	41	0.640	0.335	0.0140

mole-% Li_3AlF_6, respectively. For the former plot, a constant CO_2 content of 45% was maintained on the anode and in the latter instance, a mixture containing 40% was used.

The constants for the Tafel equations derived from the η — log i curves are summarized in Table II. The exchange current obtained by extrapolation of the Tafel curve to $\eta = 0$, is given in the fifth column of Table II.

The onset of an anode effect using the Na_2LiAlF_6 solvent at a temperature of 1010°C was observed when the current density reached 14.5 amp cm^{-2} while for the equimolar lithium-sodium cryolite solvent the effect occurred at 13 amp cm^{-2}. At a lower temperature, 960°C, in the former electrolyte the maximum current density reproduced for the normal anodic process was found to be 14 amp cm^{-2}.

Discussion

Comparison of Anodic Overpotentials in Different Electrolytes

From the results in Figures 2, 4, and 6, it can be concluded that variation in the composition of the cryolitic solvent for alumina in the Hall-Heroult cell has negligible effect upon the anodic overpotential by comparison with the reproducibility between different experiments.[4] This conclusion is exemplified by the data in Table III where the overpotential results for the different cryolite mixtures are compared with those obtained with pure Na_3AlF_6 solvent. The anode gas compositions for all the experimental runs cited in Table III were within the range 62 ± 5% CO_2. The current densities at which the anode effect occurs and the limiting current densities are also listed in Table III.

TABLE III
Comparison of Anode Overpotentials for Several Electrolytes Containing 17.1 Mole-% Al_2O_3 at 1010°C

Solvent electrolyte	Overpotentials, volts, at given current densities, amp cm^{-2} 0.02	0.05	0.1	0.2	0.5	c.d. at anode effect, amp cm^{-2}	i_L amp cm^{-2}
Na_3AlF_6	0.04	0.10	0.195	0.29	0.44	13.5	6.3
$3Na_3AlF_6$ + CaF_2	0.04	0.11	0.210	0.30	0.44	13.5	5.8
$2Na_3AlF_6$ + Li_3AlF_6	0.04	0.10	0.195	0.30	0.44	14.5	6.1
Na_3AlF_6 + Li_3AlF_6	0.05	0.12	0.220	0.31	0.45	13.0	5.9

Therefore, in the composition range investigated, there is no effect induced on the overpotential for the anode process occurring at a particular current density when additives are introduced into the electrolyte. Similarly, both the current density at which the anode effect occurs and the limiting current are substantially in agreement and hence independent of the cryolite solvent at constant mole fraction of Al_2O_3 in the melt. The overpotential does decrease with increasing concentration of Al_2O_3.[4]

In the region of the limiting c.d. the overpotential is largely determined by concentration overpotential, and therefore the limiting current may be expressed by the equation

$$i_L = DzFc/\delta$$

where D is the diffusion coefficient, z the charge of the anion of concentration c, F represents the Faraday, and δ the thickness of the diffusion layer. It is reasonable to assume that at the same temperature all other physical conditions being equal, the limiting current in the different electrolytes will be proportional to the concentration of reacting species. From the good agreement among the experimental values of i_L in Table III, it is clear that the concentration of the ion participating in the anode reaction is constant and therefore dependent on the alumina concentration and not the solvent composition. The results obtained also indicate that there is no change in the ratio of diffusion coefficient to thickness of diffusion layer over the temperature range studied since, for a particular electrolytic mixture the limiting c.d.'s determined at 960 and 1010°C agree within the experimental error.

Effect of Anodic Gas Composition on Overpotential

In the system Na_3AlF_6-Al_2O_3 it has been found that the effect of different anode gases was most evident in the value of the i_0.[7] The slope of the plot of log P_{CO_2} versus log i_0 was approximately 0.33, but in many cases there was an uncertainty associated with this relationship.

A plot of log P_{CO_2} against log i_0 for the three systems studied at 1010°C in this work is presented in Figure 8. For the solvent $3Na_3AlF_6 + CaF_2$ the best location of the curve is doubtful, although the value of $(d \log i_0/d \log P_{CO_2})$ probably lies within the range 0.18 to 0.40. In the electrolyte Na_3LiAlF_6($d \log i/d \log P_{CO_2}$) is equal to 0.30 while for $(NaLi)_{3/2}AlF_6$ the slope is 0.29. The range of these slopes is similar to that found for $Na_3AlF_6 + Al_2O_3$ systems. The relationship of gas composition is probably independent of the solvent. Until more experimental data have been obtained, the significance of the relationship, $i_0 \propto P_{CO_2}^{1/3}$ does not justify theoretical interpretation. At present such a formulation gives a good indication of the effect of anode gas on the exchange current.

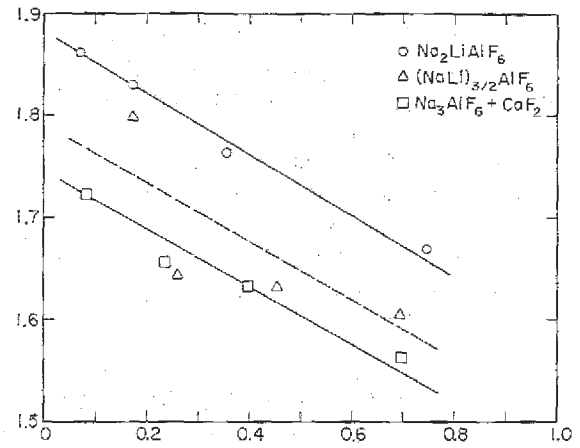

Fig. 8. Plot of log (exchange current) against log (partial pressure of CO_2) in anode gas. Ordinate: $-\log i_0$. Abscissa: $-\log P_{CO_2}$.

Temperature Dependence of Overpotential

Assuming the heat of activation (ΔH) of the rate-controlling reaction is independent of temperature, then at constant overpotential the temperature dependence of current density may be expressed by

$$\left[\frac{d \ln i}{d\ (1/T)}\right]_\eta = -\frac{\Delta H}{R}$$

The exchange currents, i.e., $\eta = 0$, for the limited temperature range of this investigation are plotted against the reciprocal absolute temperature in Figure 9. The values of ΔH thus determined are 14.5 ± 3.0 kcal/mole for the solvent $3Na_3AlF_6 + CaF_2$; 14 ± 3 kcal/mole for $2Na_3AlF_6 + Li_3AlF_6$; and 10.5 ± 2 kcal/mole for the equimolar mixture of $Na_3AlF_6 + Li_3AlF_6$. The heat of activation of this anodic reaction determined by a potentiostatic method[4] was found to be 12.9 ± 1.4 kcal/mole. As expected from theoretical considerations, the overpotential at a given current density decreased with increase in temperature. In the equimolar mixture of cryolites, this decrease was 80 mv for an increase of 55° in temperature at $i = 0.2$ amp cm^{-2}.

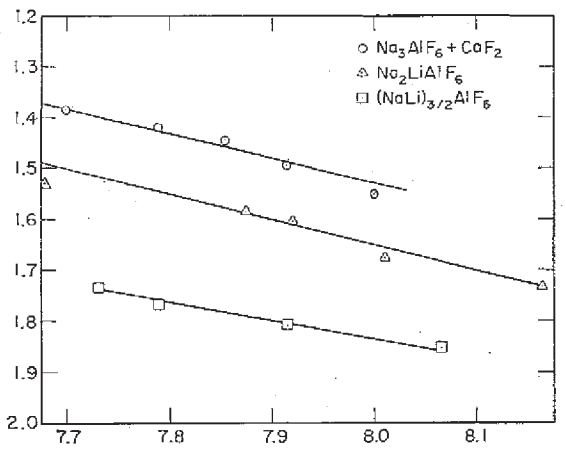

Fig. 9. The relationship between log i_0 and the reciprocal absolute temperature. Ordinate — log i_0. Abscissa: $1/T \times 10^4$ (°K)$^{-1}$.

The Anodic Reaction Mechanism

The slope of the Tafel curves is independent of the anode gas and cryolite bath composition. The measured slopes all lie within the range 0.327 ± 0.015 which is in excellent agreement with those reported earlier.[4] The present work indicates that the oxygen-containing anions are the same in each of the cryolite mixtures. Consequently, the anode reaction mechanism for the electrolytic decomposition of Al_2O_3 will be identical in each of the different supporting electrolytes. The Tafel slope is related to the symmetry factor (β) and the number of electrons (n) involved in the rate-determining step of the electrode reaction by the equation

$$\frac{d\eta}{d \log i} = 2.303(RT/n\beta F)$$

In these experiments at 1283°K,

$$n\beta = \frac{0.254}{0.327}$$

$$= 0.78$$

Since the Tafel slopes and anionic species here appear identical with those of the $Na_3AlF_6 + Al_2O_3$ system, then it is reasonable to accept the experimentally determined value for β, 0.4[4] in which case the number of electrons involved in the rate-determining equation must be 2.

In the following presentation of reaction mechanisms it has been assumed that CO_2 is the primary anode product. This assumption is consistent with the experiments of Hamlin and Richards[8] and Pearson and Waddington.[9] However, it will be seen that the acceptable mechanisms will hold equally as well for the evolution of CO.

The several possible anions resulting from the solvation of alumina, e.g., AlO_2^-, $Al_2O_2F_4^{2-}$, $AlOF_2^-$, $AlOF_3^{2-}$, etc., may be represented by the general anionic formula, $Al_xO_yF_z^{3x-2y-z}$. The following mechanisms would equally well apply to these anions, but for simplicity AlO_2^- has been used as a general example.

Mechanism I: Consider the consecutive processes to be

$$AlO_2^- \underset{k_{-1}}{\overset{k_1}{\rightleftharpoons}} AlO^+ + O^{2-}$$

(I)

$$O^{2-} + C \underset{k_{-2}}{\overset{k_2}{\rightleftharpoons}} C^*O + 2e$$

(II)

$$2C^*O \underset{k_{-3}}{\overset{k_3}{\rightleftharpoons}} C + CO_2$$

(III)

Assuming reaction II is rate determining and the surface coverage by C*O is negligible, then it can be shown[10–12] that the expression for the forward rate v of the overall electrode reaction is

$$v = \frac{k_1}{k_{-1}} k_2 \frac{C_{AlO_2^-}}{C_{AlO^+}} e^{2\eta\beta F/RT}$$

hence

$$i = 2k_2K_1F \frac{C_{AlO_2^-}}{C_{AlO^+}} e^{2\eta\beta F/RT}$$

for which the Tafel slope would be

$$\frac{\partial\eta}{\partial \ln i} = \frac{RT}{2\beta F}$$

Considering the case where reaction III is rate determining, i.e., the slow desorption of chemisorbed oxide, then the rate expression would be

$$i = 4k_3K_1K_2F \frac{C^2_{AlO_2^-}}{C^2_{AlO^+}} e^{4\eta F/RT}$$

and the Tafel slope would be given by

$$\frac{\partial\eta}{\partial \ln i} = \frac{RT}{4F}$$

Thus, in these kinetics, reaction II is the only rate-determining step consistent with experiment.

Mechanism II: Consider the following mechanism of consecutive discharge of oxygen ions:

$$AlO_2^- + C \underset{k_{-4}}{\overset{k_4}{\rightleftharpoons}} AlO^+ + C^*O + 2e \qquad \text{(IV)}$$

$$AlO_2^- + C^*O \underset{k_{-5}}{\overset{k_5}{\rightleftharpoons}} CO_2 + AlO^+ + 2e \qquad \text{(V)}$$

For reaction IV as the rate-controlling process the rate equation is

$$i = 2k_4F \cdot C_{AlO_2^-} \cdot e^{2\eta\beta F/RT}$$

and

$$\frac{\partial\eta}{\partial \ln i} = \frac{RT}{2\beta F}$$

If reaction V is the rate-determining step it can be shown that

$$i = 2k_5K_4F \frac{C^2_{AlO_2^-}}{C_{AlO^+}} e^{2(1+\beta)\eta F/RT}$$

Hence,

$$\frac{\partial\eta}{\partial \ln i} = \frac{RT}{2(1+\beta)F}$$

Thus, for mechanism II, reaction IV is the only acceptable rate-controlling step, in accordance with the experimentally measured Tafel slopes.

It is apparent that reaction IV does not basically differ from reaction II of mechanism I. For each of the anions mentioned above, thermodynamically consistent mechanisms for both the anodic process and overall electrolysis can be formulated. By comparison of the theoretical rate equations with the Tafel slopes, the rate-determining step in every case is the same, i.e., a two-electron transfer during the initial discharge of oxide or oxyfluoride ions onto the carbon surface to form an intermediate chemisorbed complex C*O. Subsequent reaction and desorption leads to the evolution of CO_2.

The authors wish to acknowledge the assistance of Mr. J. S. Berry, Jr., in the construction of apparatus and Mr. C. C. Nance in the experimental operation. We are grateful for the permission of Reynolds Metals Co. to publish this work.

References

1. Antipin, L. N., and A. N. Khudyakov, *Zh. Prikl. Khim.*, 29, 908 (1956).
2. Mashovets, V. P., and A. A. Revazyan, *Zh. Prikl. Khim.*, 31, 571 (1958).
3. Richards, N. E., *J. Phys. Chem.*, in press.
4. Richards, N. E., and B. J. Welch, *J. Electrochem. Soc.*, in press.
5. Tafel, J., *Z. Physik. Chem.*, 50, 641 (1905).
6. Janz, G. J., and Fumihiko Saegusa, *J. Electrochem. Soc.*, 108, 663 (1961).
7. Welch, B. J., and N. E. Richards, unpublished data.
8. Hamlin, J. D., and N. E. Richards, AIME International Symposium on Extractive Metallurgy of Aluminum, New York, 1962.
9. Pearson, T. G., and J. Waddington, *Disc. Faraday Soc.*, 1, 307 (1947).
10. Bockris, J. O'M., *J. Chem. Phys.*, 24, 817 (1956).
11. Christiansen, A., *Z. Physik. Chem.*, B33, 145 (1936).
12. Parsons, R., *Trans. Faraday Soc.*, 47, 1332 (1951).

Discussion

W. E. Haupin (*Alcoa Research Labs, New Kensington, Pa.*): Much of the straight-line part of the Tafel curves presented is below the currents used in commercial cells. There appears to be a change in the Tafel slope at about 0.5 amp/cm². Does this indicate that the reaction you postulate may not apply at current densities used in practical operation?

B. J. Welch: Much of the data are within the range of practical operation experienced, particularly for Soderberg cells, e.g., the current densities shown in the abscissae are in the range, 10^{-3} to 2 amp cm^{-2}. The deviation from the Tafel line at the higher current densities is due to concentration polarization being superimposed on activation overpotential. The slope of the curve at these higher c.d.'s is continually changing and is not indicative of another process.